# Fischer−Tropsch Synthesis with Cobalt Catalysts Supported on Mesoporous Silica for Efficient Production of Diesel Fuel Fraction

Yasuo Ohtsuka,* Takashi Arai, Satoshi Takasaki, and Naoto Tsubouchi

*Research Center for Sustainable Materials Engineering, Institute of Multidisciplinary Research for Advanced Materials, Tohoku University, Katahira, Aoba-ku, Sendai 980-8577, Japan*

*Received October 15, 2002*

Fischer−Tropsch (FT) synthesis with Co catalysts supported on mesoporous silica (SBA-15) with narrow pore size distribution has been carried out with a fixed bed stainless steel reactor at 503 K and 2.0 MPa. When 20 mass % Co is supported on SBA-15 with an average pore diameter of 8.6 nm by using an ethanol solution of Co acetate, nitrate, or an equimolar mixture of these compounds, denoted as Co(20A), Co(20N), or Co(10A+10N), respectively, the Co(20A) is almost inactive in FT synthesis, whereas the Co(20N) and Co(10A+10N) drastically enhance CO conversion, which reaches 85−90%. Such differences arise partly from the formation of less or more reducible Co species. The latter two catalysts show selectivity to $C_{10}$−$C_{20}$ hydrocarbons of 30−32 C-mol % and provide high space-time yields of this fraction as the main component of diesel fuel, 260−270 g-C/kg-catalyst·h. The yield with the Co(20N) catalyst depends on the amount and has a maximal value of 350 g-C/kg-catalyst·h. The $N_2$ adsorption, X-ray diffraction, and temperature-programmed reduction measurements reveal that pore structures and dispersion states of Co(20N) and Co(10A+10N) catalysts are not changed significantly, even after FT synthesis and subsequent air calcination at 773 K.

## Introduction

Fischer−Tropsch (FT) synthesis has recently attracted renewed interest, because a high quality diesel oil fraction without any sulfur and aromatic compounds can be produced from syngas derived from natural gas.[1−5] Cobalt-based catalysts loaded on different supports, such as $SiO_2$, $Al_2O_3$, and $TiO_2$, have been widely used in this reaction to form long-chain aliphatic hydrocarbons.[2,6,7] It has been reported that the specific rate of CO conversion increases linearly with increasing dispersion of metallic Co, irrespective of the kind of support, under conditions that favor chain growth reactions, and that selectivity to $C_5$+ hydrocarbons relates with the diffusion of reaction intermediates within the pores of the catalyst support.[6,8,9] These observations suggest that physical structures of the support, for example surface area for catalyst dispersion and pore properties for product diffusion, are one of the key factors for efficient production of long-chain aliphatic hydrocarbons, such as $C_{10}$−$C_{20}$ paraffins, as the main component of diesel oil.

As is well-known, mesoporous silica materials recently developed, such as MCM-41,[10] FSM-16,[11] and SBA-15,[12] have unique physical structures: narrow pore size distribution, large pore diameters in the range of 2−30 nm, high surface areas reaching 1000 $m^2$/g, and large pore volumes of 1−2 $cm^3$/g, compared with those of conventional $SiO_2$ supports. Thus, the present authors have been working on the utilization of such mesoporous materials as catalyst supports in FT synthesis[13−16] and have shown that, when 20 mass % Co is incorporated into SBA-15 with different pore diameters of 3−15 nm,[13] the Co/SBA-15 catalyst with an average diameter of about 8.5 nm exhibits the highest activity at 523 K and 2.0 MPa, although $CH_4$ selectivity is large due probably to the high temperature.[14] The present work thus

* Author to whom correspondence should be addressed. E-mail: ohtsukay@tagen.tohoku.ac.jp.

(1) Xu, L.; Bao, S.; O'Brien, R. J.; Raje, A.; Davis, B. H. *CHEMTECH* **1998**, 47−53.
(2) Schulz, H. *Appl. Catal. A: General* **1999**, *186*, 3−12.
(3) Davis, B. H. *Fuel Process. Technol.* **2001**, *71*, 157−166.
(4) Iglesia, E. *Prepr. Pap.—Am. Chem. Soc., Div. Fuel. Chem.* **2002**, *47* (1), 128−131.
(5) Dry, M. E. *Catal. Today* **2002**, *71*, 227−241.
(6) Iglesia, E. *Appl. Catal. A: General* **1997**, *161*, 59−78.
(7) Van der Laan, G. P.; Beenackers, A. A. C. M. *Catal. Rev. Sci. Eng.* **1999**, *41*, 255−318.
(8) Iglesia, E.; Soled, S. L.; Fiato, R. A. *J. Catal.* **1992**, *137*, 212−224.
(9) Iglesia, E.; Reynes, S. C.; Madon, R. J.; Soled, S. L. *Adv. Catal.* **1993**, *39*, 239.
(10) Kresge, C. T.; Leonowicz, M. E.; Roth, W. J.; Vartuli, J. C.; Beck, J. S. *Nature* **1992**, *359*, 710−712.
(11) Inagaki, S.; Fukushima, Y.; Kuroda, K. *J. Chem. Soc., Chem. Commun.* **1993**, 680−681.
(12) Zhao, E.; Feng, J.; Huo, Q.; Melosh, N.; Fredrickson, G.; Chmelka, B.; Stucky, G. *Science* **1998**, *279*, 548−552.
(13) Wang, Y.; Noguchi, M.; Takahashi, Y.; Ohtsuka, Y. *Catal. Today* **2001**, *68*, 3−9.
(14) Wang, Y.; Takahashi, Y.; Noguchi, M.; Ohtsuka, Y. *Proceedings of the 7th China-Japan Symposium on Coal and $C_1$ Chemistry* (Hainan Island, China), 2001; pp 65−68.
(15) Mal, N. K.; Ohtsuka, Y. Proceedings of the *Fourth Tokyo Conference of Advanced Catalytic Science and Technology* (Tokyo, Japan), 2002; p 336.
(16) Ohtsuka, Y.; Arai, T.; Takasaki, S.; Tsubouchi, N. *Prepr. Pap.—Am. Chem. Soc., Div. Fuel Chem.* **2002**, *47* (2), 492−493.

10.1021/ef020235r CCC: $25.00 
Published on Web 05/08/2003

focuses on FT synthesis at a low temperature of 503 K to increase $C_5$+ selectivity. The objectives are to examine the effects of Co precursor and catalyst amount on the performances of Co/SBA-15 catalysts, in particular, space-time yield (denoted as STY) of $C_{10}-C_{20}$ hydrocarbons, and to make clear the structural stability after reaction from a practical point of view.

## Experimental Section

**Synthesis of Mesoporous Silica.** SBA-15 was synthesized in a manner similar to that reported earlier.[12] The procedure has been described in detail elsewhere[13] and thus is simply explained below. An acidic aqueous mixture of a triblock copolymer (Aldrich), poly(ethylene oxide)−poly(propylene oxide)−poly(ethylene oxide) ($EO_{20}PO_{70}EO_{20}$), trimethylbenzene, and tetraethyl orthosilicate was first heated at 308 K for 24 h, followed by postsynthesis treatment at 370 K. Then, as-synthesized SBA-15 was separated by filtration, followed by repeated washing with distilled water, and subsequently dried at room temperature under vacuum; it was finally calcined in air at 773 K for 6 h. The calcined SBA-15 was characterized by the $N_2$ adsorption measurements and used as a support for the Co catalyst.

**Catalyst Addition and Characterization.** Co catalysts were loaded on the SBA-15 with an average pore diameter of 8.6 nm by the impregnation method[13] using an ethanol solution of $Co(CH_3COO)_2$, $Co(NO_3)_2$, or the equimolar mixture; these were denoted as Co(A), Co(N), or Co(A+N), respectively. After removal of ethanol, the resulting samples were again calcined at 773 K under flowing air. Loading of Co metal is expressed in $x$ and $y$ mass % of Co($x$A+$y$N); for example, Co(10A+10N) denotes 10 mass % Co from $Co(CH_3COO)_2$ and 10 mass % Co from $Co(NO_3)_2$, and Co(20N) means 20 mass % Co from $Co(NO_3)_2$ alone.

All of the Co/SBA-15 catalysts after air calcination were subjected to X-ray diffraction (XRD) and $N_2$ adsorption measurements. The average crystalline size of $Co_3O_4$ identified by XRD was calculated by the Debye−Scherrer method. Pore size distribution and specific surface area were determined by the BJH and BET methods, respectively. The average pore diameter of each catalyst was estimated by using total volume and surface area of mesopores on the assumption that they are cylindrical.[12] To examine chemical forms and reducibility of Co species in some catalysts, the temperature-programmed reduction (TPR) measurements were made by heating at 10 K/min up to 1273 K in an atmospheric stream of $H_2$ diluted with Ar, and the changes in $H_2$ concentration were on-line monitored with a gas chromatograph.

**FT Runs and Product Analysis.** FT runs were carried out with a high-pressure gas-phase reaction system including a cylindrical stainless reactor (8-mm i.d., 330 mm long).[13] About 0.1−0.5 g of the catalyst charged into the reactor was first pretreated with atmospheric $H_2$ for 12 h at 673 K and then cooled to 373 K. After replacement of the $H_2$ with a pressurized mixture of $H_2$ and CO with a molar ratio of 2:1, the reactor was finally heated at 3 K/min up to the reaction temperature, a small amount of Ar as an internal standard being included in the mixed gas. After a predetermined soaking time, the reactor was quenched to room temperature. Catalyst amount ($W$), $W/F$ ($F$, feed rate), reaction temperature, and pressure were 0.50 g, 4.0 g h mol$^{-1}$, 503 K, and 2.0 MPa, respectively, unless otherwise stated. The temperature was controlled and measured with a thermocouple inserted into the catalyst bed.

With product analysis, $C_1-C_5$ hydrocarbons in the effluent after recovery of liquid products were on-line analyzed with a high-speed micro GC. Liquid products were recovered with three kinds of traps held in the range of room temperature to 77 K, and $C_6-C_{28}$ hydrocarbons in them were determined with a capillary GC-MS. Waxy materials remaining in the catalyst recovered after reaction were detected by the conventional elemental analyzer. The catalyst was also analyzed by XRD and $N_2$ adsorption measurements, as mentioned above.

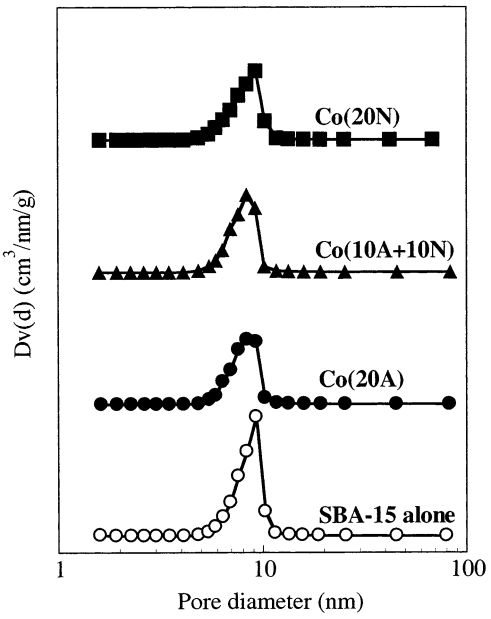


**Figure 1.** Pore size distribution for SBA-15 support and Co/SBA-15 catalysts.

**Table 1. Characterization Results of Co/SBA-15 Catalysts**

| catalyst name | Co(A) (mass%) | Co(N) (mass%) | $D_{av}$[a] (nm) | $V_p$[b] ($cm^3/g$) | $S_{BET}$[c] ($m^2/g$) | $D(Co_3O_4)$[d] (nm) |
|---|---|---|---|---|---|---|
| | 0 | 0 | 8.6 | 1.9 | 880 | |
| Co(10N) | 0 | 10 | 8.6 | 1.6 | 720 | 12 |
| Co(20N) | 0 | 20 | 8.5 | 1.3 | 590 | 20 |
| Co(10A+10N) | 10 | 10 | 8.2 | 1.4 | 530 | 9.1 |
| Co(20A) | 20 | 0 | 8.3 | 1.3 | 460 | n.d.[e] |

[a] Average pore diameter. [b] Pore volume. [c] BET surface area. [d] Average crystalline size of $Co_3O_4$. [e] No species detectable.

## Results

**Properties and Structures of Co/SBA-15 Catalysts.** Figure 1 shows typical profiles for the pore size distribution of SBA-15 support and three kinds of Co/SBA-15 catalysts. As expected, all of the samples used exhibited the narrow size distribution. The support alone provided an asymmetric, sharp peak at 9.3 nm. Although the peak position was almost unchanged by Co impregnation, the height lowered, irrespective of kind of precursor salt, because Co oxide was held inside the mesopores.

Table 1 summarizes pore properties and surface areas of all the catalysts used. The SBA-15 support had an average pore diameter ($D_{av}$) of 8.6 nm, which was slightly reduced to 8.2−8.5 nm at total Co loading of 20 mass %. Pore volume and BET surface area of the support were 1.9 $cm^3/g$ and 880 $m^2/g$, respectively. The addition of 10−20 mass % Co decreased the volume and area to 1.3−1.6 $cm^3/g$ and 460−720 $m^2/g$, respectively, and the extent of the decrease was higher at larger Co loading, showing the presence of larger amounts of Co particles within the mesopores.

When four kinds of Co/SBA-15 catalysts were subjected to XRD measurements, no diffraction lines of Co

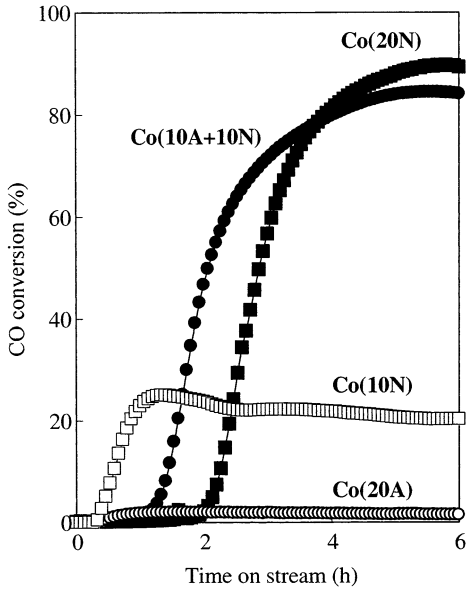


**Figure 2.** CO conversion against time on stream in FT synthesis at 503 K and 2.0 MPa.

species were detectable with Co(20A), whereas weak XRD peaks of $Co_3O_4$ appeared with Co(10N), Co(10A+10N), and Co(20N), and the peak intensities were larger with Co(20N). These observations show that Co species from the Co(20A) are less crystallized. As summarized in Table 1, the average crystalline sizes of $Co_3O_4$ estimated were 12, 9.1, and 20 nm for the Co(10N), Co(10A+10N), and Co(20N), respectively. Since these values were slightly larger than the corresponding $D_{av}$, part of the $Co_3O_4$ particles formed from these three catalysts may be present outside the mesopores.

**Performances of Co/SBA-15 Catalysts in FT Synthesis.** Figure 2 shows CO conversion at 503 K against time on stream. The conversion was only 2% on the Co(20A), which was thus almost inactive. On the other hand, the Co(10A+10N) and Co(20N) were quite active, and CO conversions after apparent induction periods increased steeply with increasing time and reached 84−89% at a steady state after 6 h. The period may be regarded mainly as the time required for replacing the dead volume up to micro GC with unreacted syngas. As is seen in Figure 2, the activity of the Co(N) catalyst depended strongly on Co loading, and CO conversion after 6 h reaction decreased to 20 % at smaller loading of 10 mass %. The shorter induction period was observed with the Co(10N), due possibly to the lower conversion. It should be noted that the conversion on the Co(10A+10N), 84%, is much higher than the sum (22%) of those observed with the Co(20A) and Co(10N); in other words, the synergistic effect exists with the activity of the Co(10A+10N) catalyst.

Time changes in yields of $CH_4$ and $C_2-C_4$ hydrocarbons with Co(10A+10N) are provided in Figure 3, where the values are calculated by dividing the molar amount of $CH_4$ or $C_2-C_4$ fraction by that of CO converted and seem unreliable at the beginning of reaction; that is, within 1 h, due to very low CO conversion. The yields were larger in the lower conversion region but decreased with time to reach stable values (4−8 mol %) after 3 h. Almost the same profiles were observed for the Co(20N).

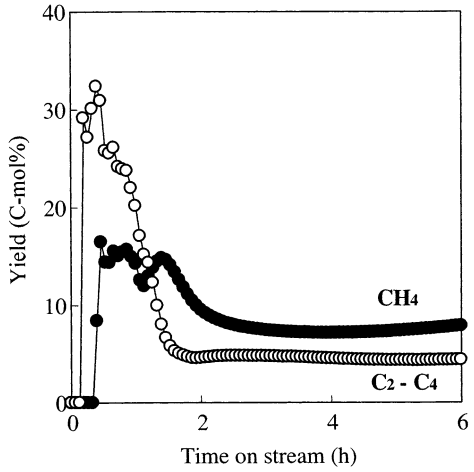


**Figure 3.** Time changes in yields of $CH_4$ and $C_2-C_4$ hydrocarbons at 503 K with Co(10A+10N)/SBA-15 catalyst.

**Table 2. Hydrocarbon Products in FT Synthesis with Co/SBA-15 Catalysts**

| | selectivity (C-mol %) | | | | |
|---|---|---|---|---|---|
| catalyst name | $C_5-C_9$ | $C_{10}-C_{20}$ | $C_{21}+^c$ | $\alpha^a$ | STY of $C_{10}-C_{20}{}^b$ (g-C/kg-catalyst·h) |
| Co(10N) | 30 | 30 | 9 | 0.87 | 58 |
| Co(20N) | 27 | 30 | 15 | 0.92 | 270 |
| Co(10A+10N) | 24 | 32 | 16 | 0.93 | 260 |

[a] Chain growth probability. [b] Space time yield. [c] $C_{21}-C_{28}$ plus waxy materials.

The results for liquid hydrocarbons produced over the Co(10N), Co(20N), and Co(10A+10N) catalysts are summarized in Table 2, where product selectivity for $C_5-C_9$, $C_{10}-C_{20}$, and $C_{21}+$ ($C_{21}-C_{28}$ plus waxy materials remaining in recovered catalyst) fractions is expressed in C-mol % as the mean value for 6 h reaction. A small amount of $CO_2$ was formed for the Co(20N) alone. Selectivity to $C_5-C_9$ was larger with the Co(10N), whereas selectivity to $C_{10}-C_{20}$ was almost independent of the kind of catalyst and ranged 30−32 C-mol %, and the $C_{21}+$ fraction was larger with the Co(20N) and Co(10A+10N) catalysts, which roughly followed the Schultz−Flory distribution and lead to higher chain growth probabilities ($\alpha$) of 0.92−0.93, though the linearity was not so good. Table 2 also shows space-time yield (denoted as STY) of $C_{10}-C_{20}$ hydrocarbons as the main components of diesel fuel, the value being estimated by using CO conversion after 6 h and selectivity to this fraction provided in Table 2. The STY was 58 g-C/kg-catalyst·h with the Co(10N), whereas it was as high as 260−270 g-C/kg-catalyst·h with the Co(10A+10N) and Co(20N).

The effect of *W*/*F* on catalytic performance of the Co(20N) at 503 K is provided in Figure 4, where the *W* alone is varied while keeping the *F* constant. CO conversion after 6 h increased monotonically with increasing *W*/*F*, that is, contact time between catalyst and syngas. With product distribution, selectivity to long-chain hydrocarbons, such as $C_{10}-C_{20}$ or $C_{21}+$ fraction, was higher at larger *W*/*F*. Consequently, the STY of the former fraction showed a maximal value of 350 g-C/kg-catalyst·h at *W*/*F* of 2.4 g·h/mol. Under these conditions, the productivity of $C_5-C_{20}$ hydrocarbons reached 710 g-C/kg-catalyst·h.

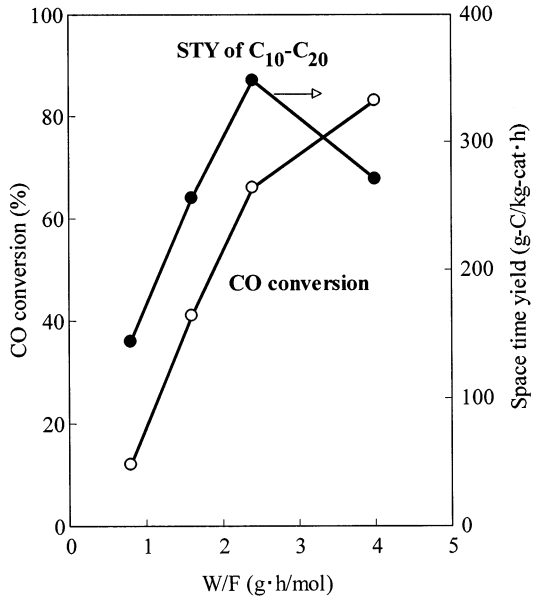


**Figure 4.** Effect of *W/F* on FT performance of Co(20N)/SBA-15 catalyst at 503 K.

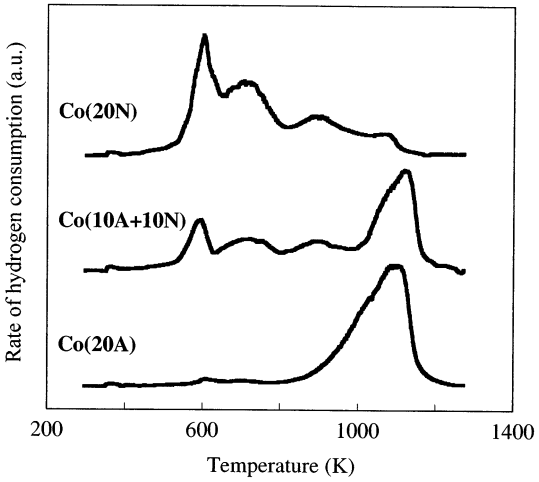


**Figure 5.** TPR profiles for three kinds of Co/SBA-15 catalysts.

**Reducibility of Co/SBA-15 Catalysts.** As is seen in Figure 2, the Co(20A) was almost inactive, but contrarily the Co(10A+10N) and Co(20N) were quite active. To make clear this difference, TPR measurements of the fresh catalysts after air calcination were made. The profiles are shown in Figure 5. The Co(20A) had a broad peak at 900−1200 K. The peak may be identified to $H_2$ consumption by reduction of $Co_2SiO_4$ to metallic Co.[17] On the other hand, the Co(20N) showed the main and shoulder peaks at 600 and 710 K, respectively, followed by two weak ones after 800 K. The former two peaks can be attributed to the reduction of $Co_3O_4$ to CoO and subsequently to metallic Co,[18] which means that $Co_3O_4$ is the predominant species in the fresh Co(20N) catalyst. The presence of this species agreed with the XRD results (Table 1). The Co(10A+10N) provided the intermediate profile between the above two—in other words, the coexistence of $Co_3O_4$ and $Co_2SiO_4$. The former species was also detectable by XRD (Table 1), but any diffraction lines of $Co_2SiO_4$ were not observed in the Co(10A+10N) and Co(20A) as a result probably of the amorphous state.

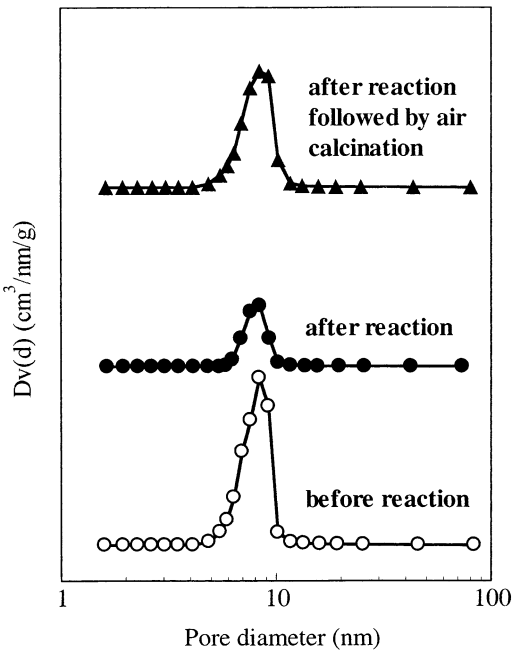


**Figure 6.** Comparison of pore size distribution for Co(10A+10N)/SBA-15 catalyst before and after FT synthesis.

Because all of the fresh catalysts after air calcination are pretreated with $H_2$ at 673 K for 12 h before FT runs, as described in the Experimental Section, the results obtained in Figure 5 show that $Co_3O_4$ in the Co(20N) and Co(10A+10N) can be reduced to metallic Co, whereas $Co_2SiO_4$ as the major species in the Co(20A) is not reduced and still remained even after $H_2$ pretreatment. It is likely that such differences in chemical forms of Co species and their consequent reducibility to metallic Co can account for the distinct activity observed with the Co(20A) and Co(20N) catalysts. Although the proportion of the readily reducible $Co_3O_4$ was smaller in the Co(10A+10N) than in the Co(20N), their performances were almost the same (Figure 2 and Table 2). The reason is not clear at present and should be clarified in future work. It has been reported that Co acetate supported on commercial $SiO_2$ support is catalytically activated in FT synthesis in the presence of Co nitrate.[19]

**Structural Stability of Co/SBA-15 Catalysts with High Performances.** Figure 6 shows the pore distribution of the used Co(10A+10N) catalyst after reaction and subsequent solvent washing. The peak height was reduced to be one-third of that before reaction, which means a considerable decrease in pore volume. Almost the same distribution was observed with the used Co(20N). One may expect that such a reduction is caused by the retention of significant amounts of waxy materials inside the mesopores. To make this point clear, the used Co(10A+10N) and Co(20N) were subjected to the XRD measurements. Since both catalysts showed almost the same XRD patterns, the results for Co(10A+10N) alone are provided in Figure 7, where the profile for the sample before reaction, that is, the fresh Co(10A+10N) after air calcination, is also shown for a reference. The

(17) Rosynek, M. P.; Polansky, C. A. *Appl. Catal.* **1991**, *73*, 97−112.
(18) Ming, H.; Baker, B. G. *Appl. Catal. A: General* **1995**, *123*, 23−36.
(19) Sun, S.; Tsubaki, N.; Fujimoto, K. *Appl. Catal. A: General* **2000**, *202*, 121−131.

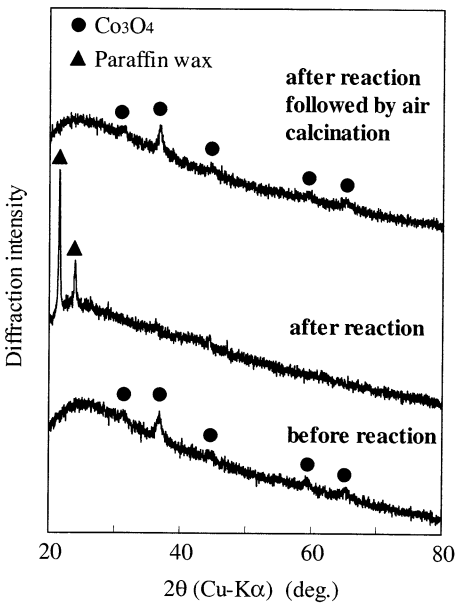


**Figure 7.** Changes in XRD profiles for Co(10A+10N)/SBA-15 catalyst before and after FT synthesis.

profile after reaction confirmed the presence of very sharp XRD peaks attributable to long-chain saturated hydrocarbons (paraffin wax). With Co species, the weak XRD signals of $Co_3O_4$ observed for the fresh catalyst disappeared after the reaction, but no diffraction lines due to metallic Co appeared. Although the reason for the difference in the XRD intensities of $Co_3O_4$ and metallic Co is not clear, the same phenomenon was also observed with the Co(20N) catalyst. The absence of any XRD signals of metallic Co with the Co(10A+10N) and Co(20N) indicates that the Co is finely dispersed even after FT synthesis.

When the used Co(10A+10N) was calcined again at 773 K, the XRD signals of the wax disappeared completely, and $Co_3O_4$ appeared again (Figure 7), as is to be expected. The average crystalline size of the Co species was estimated to be 12 nm, which was nearly equal to that (9 nm) for the fresh catalyst (Table 1). In addition, the recalcination restored the pore distribution to almost the same state as that of the fresh catalyst, as is seen in Figure 6. Such changes in both XRD profiles and pore size distribution before and after reaction followed by air calcination were observed, quite similarly with the Co(20N) catalyst. Thus, these observations show that pore structures and dispersion states of the Co(10A+10N) and Co(20N) with high performances are almost unchanged before and after FT synthesis, even when these catalysts are exposed to hot gas including $H_2O$ and $CO_2$ evolved from the wax upon recalcination at 773 K. Such a structural stability may originate from thick walls of the mesopores in SBA-15, compared with those for other mesoporous silica materials,[12] and it suggests that catalytic performances of the Co(20N) and Co(10A+10N) are also stable, though should be confirmed in the future study.

## Discussion

Although many publications have reported on synthesis, characterization, and catalytic applications of mesoporous silica materials with narrow pore size distribution, only quite limited information on FT synthesis with them as catalyst supports, except for the present authors' work,[13−16] has recently been provided.[20−22] When 15 mass % Co supported on hexagonal mesoporous silica (HMS),[21] synthesized by a method different from that for MCM-41, with the pore size and volume of 3 nm and 0.4 $cm^3/g$, respectively, was used in FT synthesis at 503 K and 2.0 MPa, high CO conversion of 88% was observed and long-chain waxy hydrocarbons were mainly formed. Compared with this result, the present Co(20N) and Co(10A+10N) showed almost the same conversions of 84−89% (Figure 2), whereas these catalysts provided lower selectivity to the wax fraction, in other words, higher selectivity to $C_{10}$−$C_{20}$ hydrocarbons (Table 2), despite reaction conditions quite similar to those above. As shown in Table 1, the Co(20N) and Co(10A+10N) catalysts had larger pore diameters (8.2−8.5 nm) and consequently larger pore volumes (1.3−1.4 $cm^3/g$) than the Co/HMS catalyst. Such pore properties may provide longer residence times of long-chain hydrocarbons inside the mesopores, which may lead to secondary cracking reactions of the wax to increase the diesel oil fraction.

It is of interest to compare FT performances of Co catalysts supported on mesoporous silica materials and conventional $SiO_2$ supports. Higher CO conversion at 510 K and 2.1 MPa was reported for Co catalysts on a uniform mesoporous silica (SCMM) with average pore diameter ($D_{av}$) of 3.6 nm than on commercial $SiO_2$ gel with $D_{av}$ of >10 nm.[20] The low conversion of 30% was also observed with a Co catalyst supported on conventional $SiO_2$ under the present conditions. When 20 mass % Co(N) was supported on $SiO_2$ gel with $D_{av}$ of 8.7 nm, nearly equal to that in this work, though the pore volume of 1.2 $cm^3/g$ and the surface area of 270 $m^2/g$ with the gel were smaller, CO conversion in a slurry phase FT run at 503 K and 1.0 MPa under $W/F$ of 5.0 g·h/mol was 30%,[19] which was much lower than that (89%) on the present Co(20N) catalyst. Since it appears that the effects of total pressure of more than 1 MPa and reaction phase on CO conversion with Co catalyst are not significant,[19,23,24] higher CO conversion observed in this work may be ascribed not only to uniform mesopores of SBA-15 support but also to the larger pore volume and higher surface area. The latter two factors should play the crucial roles in high dispersion of high loading of Co species.[13] In fact, the average crystalline size of metallic Co on the $SiO_2$ gel was estimated to be >16 nm,[19] whereas the Co on the present SBA-15 support was too fine to be detected by XRD (Figure 7). It has also been reported that, as the pore volume of commercial $SiO_2$ support for loading 20 mass % Co(N) increases from 0.7 to 2.3 $cm^3/g$, $Co_3O_4$ species formed after calcination can be more readily reduced with $H_2$ at a lower temperature, and the degree of the reduction becomes higher.[25] Larger reducibility and higher disper-

(20) Iwasaki, T.; Reinikainen, M.; Onodera, Y.; Hayashi, H.; Ebina, T.; Nagase, T.; Torii, K.; Kataja, K.; Chatterjee, A. *Appl. Surf. Sci.* **1998**, *130*, 845−850.
(21) Yin, D.; Li, W.; Xiang, H.; Sun, Y.; Zhong, B.; Peng, S. *Microporous Mesoporous Mater.* **2001**, *47*, 15−24.
(22) Khodakov, A. Y.; Griboval-Constant, A.; Bechara, R.; Zholobenko, V. L. *J. Catal.* **2002**, *260*, 230−241.
(23) Sharma, B. K.; Sharma, M. P.; Roy, S. K.; Kumar, S.; Tendulkar, S. B.; Tambe, S. S.; Kukarni, B. D. *Fuel* **1998**, *77*, 1763−1768.
(24) Fan, L.; Han, Y. Z.; Yokota, K.; Fujimoto, K. *J. Jpn. Pet. Inst.* **1996**, *39*, 111−119.

sion of the Co(20N)/SBA-15 catalyst may account for the higher CO conversion obtained in the present study.

It has been accepted in FT synthesis that, since severe restrictions on mass transport decrease CO concentration within catalyst pores and consequently lower chain growth probability, a catalyst with moderate transport restrictions can provide optimum selectivity to $C_5+$ hydrocarbons.[6,26] When 20 mass % Co(N) was supported on $SiO_2$ gel with a different $D_{av}$ of 2−15 nm, $C_5+$ selectivity and chain grown probability tended to show maximum values at $D_{av}$ of 10 nm.[25] These results suggest that the SBA-15 support with $D_{av}$ of 8.6 nm used in the present study may be suitable for metallic Co to promote chain growth reactions, which may lead to high STY of $C_{10}-C_{20}$ hydrocarbons on the Co(20N) and Co(10A+10N) (Table 2 and Figure 4). The STY observed was 260−270 g-C/kg-catalyst·h, which was much higher than those (70−90 g-C/kg-catalyst·h)[19,25] estimated for 20 mass % Co catalysts supported on conventional $SiO_2$ supports with almost the same $D_{av}$ as in the present work, when compared under similar reaction conditions. If significant amounts of waxy materials formed with the Co(20N) and Co(10A+10N) are secondarily cracked to $C_{10}-C_{20}$ hydrocarbons within catalyst pores, the STY could be increased further. The formation of weak acid sites by incorporating $Al^{3+}$ cations into the SBA-15 support may be effective for this purpose.[21] To examine this point will be the subject of future work.

(25) Saib, A. M.; Claeys, M.; van Steen, E. *Catal. Today* **2002**, *71*, 395−402.

(26) Iglesia, E.; Soled, S. L.; Baumgartner, J. E.; Reynes, S. C. *J. Catal.* **1995**, *153*, 108−122.

## Conclusions

Gas-phase FT synthesis at 503 K and 2.0 MPa has been performed with 20 mass % Co catalysts supported on mesoporous silica (SBA-15) with an average pore diameter of 8.6 nm by the impregnation method using different precursor compounds. The conclusions are summarized as follows:

(1) Co acetate is almost inactive, whereas the catalyst from the nitrate or an equimolar mixture of both compounds works quite effectively and provides high CO conversions of 85−90%, the former ineffectiveness being ascribed to the formation of less reducible Co species.

(2) Active Co/SBA-15 catalysts achieve high space-time yields of 260−270 g-C/kg-catalyst·h for $C_{10}-C_{20}$ hydrocarbons as the main fraction of diesel oil, and the change in the catalyst amount leads to the optimum yield of 350 g-C/kg-catalyst·h.

(3) Pore structures and dispersion states of the used catalysts after FT synthesis do not change significantly, even when exposed to hot gas including $H_2O$ evolved during subsequent air calcination at 773 K.

**Acknowledgment.** The present work was supported by Research for the Future Program of Japan Society for the Promotion of Science (JSPS) under the Project "Synthesis of Ecological High Quality Transportation Fuels" (JSPS-RFTF98P01001).

EF020235R